Phytopathologia Mediterranea
The international journal of the
Mediterranean Phytopathological Union

Firenze University Press
www.fupress.com/pm

Research Papers

Nanoplate digital PCR assays for detection and quantification of *Xylella fastidiosa*

Alessandro PASSERA[1], Valentina GROSSO[2], Niccolò MIOTTI[1], Marzia ROSSATO[2], Francesca GAFFURI[3], Paola CASATI[1], Massimo DELLEDONNE[2,4], Piero Attilio BIANCO[1,5,*]

[1] *Department of Agricultural and Environmental Sciences – Production, Landscape, Agroenergy, University of Milan, Milan, Italy*
[2] *Department of Biotechnology, University of Verona, Verona, Italy*
[3] *Laboratorio del Servizio Fitosanitario, Servizio Fitosanitario Regione Lombardia, Fondazione Minoprio, Vertemate con Minoprio, Italy*
[4] *Genartis s.r.l., Verona, Italy*
[5] *Institute for Sustainable Plant Protection, National Research Council (IPSP-CNR), Turin, Italy*
*Corresponding author. E-mail: piero.bianco@unimi.it

Summary. *Xylella fastidiosa* is a fastidious Gram-negative bacterium that is associated with several important plant diseases, and is regulated as a quarantine pest in many countries where strategies are implemented to prevent its introduction and spread. To enact efficient quarantine measures, effective and early detection of the pathogen are essential, especially because global trade of goods increases the risks of introduction of alien pathogens. this study aimed to adapt two qPCR-based diagnostic methods (SYBR Green and Probe based qPCR), already in use to detect *X. fastidiosa*, for use with a nanoplate based digital PCR assay. Detection of the pathogen using the two digital PCR assays (EvaGreen- and Probe-based) was similar to standard qPCR, giving 100% sensitivity, specificity, and accuracy, while providing accurate absolute quantification of the pathogen when using experimental samples that had low concentrations of host DNA. Using undiluted plant DNA added with low concentrations of *X. fastidiosa*, only the TaqMan method maintained satisfactory performance and quantification, and is therefore preferred. These results are a first step demonstrating the usefulness of nanoplate-based digital PCR for detection of plant pathogens, which allows greater throughput than qPCR, reducing the time and cost of diagnostic assays.

Keywords. qPCR, *Nerium oleander*, TaqMan, EvaGreen, dPCR.

OPEN ACCESS

Citation: A. Passera, V. Grosso, N. Miotti, M. Rossato, F. Gaffuri, P. Casati, M. Delledonne, P.A. Bianco (2022) Nanoplate digital PCR assays for detection and quantification of *Xylella fastidiosa*. *Phytopathologia Mediterranea* 61(3): 489-503. doi: 10.36253/phyto-13803

Accepted: December 9, 2022

Published: January 13, 2023

Data Availability Statement: All relevant data are within the paper and its Supporting Information files.

Competing Interests: The Author(s) declare(s) no conflict of interest.

Editor: Anna Maria D'Onghia, CIHEAM/Mediterranean Agronomic Institute of Bari, Italy.

ORCID:
AP: 0000-0001-6928-453X
VG: 0000-0002-2983-728X
NM: 0000-0002-7633-4053
MR: 0000-0002-6101-1550
FG: 0000-0002-2132-4093
PC: 0000-0001-6152-8712
MD: 0000-0002-7100-4581
PAB: 0000-0002-9541-1923

INTRODUCTION

Xylella fastidiosa (Xf) is an important plant pathogen (Mansfield *et al.*, 2012). Xf is a Gram-negative bacterium that colonizes plants, particularly their xylem vessels, as well as insects. This pathogen is difficult to culture, which led to the species name of *fastidiosa* (Wells *et al.*, 1987). Xf can cause severe damage when introduced in new environments. The pathogen was

initially known in North and South America, associated with grapevine Pierce's disease (Davis *et al.*, 1978). However, Xf has been identified in numerous outbreaks, and many studies have determined that Xf has a wide host range, including 655 plant species in 88 families (EFSA, 2022). To date, the main crops affected by Xf are olive trees (*Olea* spp.), grapevine (*Vitis* spp.), citrus (*Citrus* spp.), coffee (*Coffea* spp.), peach (*Prunus persica*) and almond (*Prunus dulcis*) (Chang *et al.*, 1993; Rodriguez *et al.*, 2007; Saponari *et al.*, 2013; EFSA 2022), but the pathogen has also been found in forest trees, including American elm (*Ulmus americana*), American sycamore (*Platanus occidentalis*) and northern red oak (*Quercus rubra*) (Desprez-Loustau *et al.*, 2020), as well as in common ornamental, wild and crop plants including fleabane (*Erigeron* sp.), *Helichrysum stoechas*, pistachio (*Pistacia vera*), and persimmon (*Diospyros kaki*) (EFSA 2022). This host list is being often updated, as EFSA has been mandated by the European Commission to publish biannual updates of *Xylella* hosts species during 2021 to 2026.

Many asymptomatic hosts of Xf have been discovered, because the pathogen is commensalist with its host plants, and only a subset of interactions between specific hosts and clades of Xf can result in the disease development (Sicard *et al.*, 2018). This phenomenon is also because Xf is genetically diverse, and its classification has been a matter of opinion with as few as two and as many as five subspecies being recognized. Among these, three subspecies are widely supported: *Xylella fastidiosa* subsp. *fastidiosa*, *Xylella fastidiosa* subsp. *multiplex*, and *Xylella fastidiosa* subsp. *pauca* (Potnis *et al.*, 2019; Vanhove *et al.*, 2019). *Xylella fastidiosa* subsp. *pauca* is gaining importance in Europe as the cause of olive quick decline syndrome in Apulia (Saponari *et al.*, 2013; 2017).

As well as high genetic variability and wide host range, management of Xf is further complicated because the pathogen is transmitted by insect vectors, which harbour the bacterium in their foreguts (Purcell, 1979, Backus and Morgan, 2011). This is different from most other pathogens transmitted persistently, that instead perform complex molecular interactions with their insect vectors and have limited host ranges (Redak *et al.*, 2004). In practical terms, this means that sharpshooter leafhoppers (Hemiptera, Cicadellidae, Cicadellinae) or spittlebugs (Hemiptera, Cercopoidea, Aphrophoridae, Cercopidae, Clastopteridae), which are xylem-sap feeders, could potentially be Xf vectors (Frazier, 1965). The most important known vectors of Xf are *Homalodisca vitripennis* (Hemiptera, Cicadellidae) in America, and *Philaenus spumarius* (Hemiptera, Aphrophoridae) in Europe (Cornara *et al.*, 2016).

Taking these biological features of Xf into consideration, which are further complicated by ecological, social, and economic factors, introduction of Xf into new areas where novel vectors and hosts occur, can have severe consequences, leading to inclusion of Xf into the quarantine pest category (NAPPO, 2004; EPPO, 2021). The European Commission has published a list of priority regulated quarantine pests, including Xf, which every Member State must implement all possible actions to avoid introduction and spread of this organism, and formulate contingency plans, simulation exercises, and action plans for the eradication of these pests (Regulation (EU) 2016/2031).

For this reason, early and precise diagnoses of the presence of Xf are important, particularly because this pathogen causes non-specific symptoms which can be mistaken for abiotic stresses (Thorne *et al.*, 2006), particularly water or nutrient stress, and these symptoms develop months after infections (Baldi and La Porta, 2017). In the periods between infection and symptom development, the pathogen can be acquired by vectors and transmitted to new hosts, so diagnoses based on symptom observation are inefficient for the containment of the pathogen. However, Xf can be detected by molecular assays before host symptoms develop, so molecular assays have dominated diagnosis of this pathogen. These methods include traditional assays such as ELISA and conventional PCR, as well as more modern approaches such as real-time PCR (qPCR) and LAMP. The main methods for the detection of the pathogen are indicated in the standard EPPO PM 7/24 (EPPO, 2019), while in Regulation EU 2020/1201 (Annex IV) official test methods are indicated that must be used by laboratories for the identification of *X. fastidiosa* and its subspecies.

Despite being accurate and efficient, the current methods used for detection of Xf suffer from low throughput rates and being time-consuming and labour-intensive. These methods also allow precise pathogen quantification only when using standards of known concentration as references. Digital PCR (dPCR) can increase analysis throughput by removing the need for technical replicates and allowing absolute pathogen quantification without the need for reference material or standards (Selvaraj *et al.*, 2019). This reduces pathogen detection times. Early pathogen detection is important in areas where the pathogen is yet to establish, and at important entry points of plant material into a country, such as harbours and airports. In global trade, the availability of fast, reliable, and quantitative diagnostic assays for pathogens and pests has become are urgently required (Faino *et al.*, 2021), as testified by the reports of impor-

tant pests being recently found in new areas, for example *Erwinia amylovora*, another relevant bacterial pathogen, reported in Tuscany in 2020 (Migliorini et al., 2021).

The present study aimed to evaluate the performance of primers and probes currently employed for diagnosis of Xf through qPCR when used in a nanoplate-based dPCR assay, and to determine if the qPCR methods could be directly transposed to this new dPCR technology. Similar studies have been carried out to test these methods in droplet-based dPCR (Dupas *et al.*, 2019), but considering the technical differences between droplet- and nanoplate-based dPCR, an entirely separate set of tests for initial validation of these methods in nanoplate-based dPCR was necessary. All tests were carried out on experimental samples obtained by adding known quantities of DNA from Xf subsp. *fastidiosa*, Xf subsp. *multiplex*, or Xf subsp. *pauca* in the nucleic acid extracts from healthy plants of *Nerium oleander,* an ornamental host of Xf. These tests underwent preliminary validation by comparison with the current qPCR assays.

MATERIALS AND METHODS

Bacterial strains and DNA used in this study

Total nucleic acids from three *X. fastidiosa* strains and one strain of a non-target, non-pathogenic *Pseudomonas syringae* pv. *syringae,* belonging to a genus commonly found in healthy plant tissues, were used in this study.

The nucleic acids of pure cultures of *X. fastidiosa* subsp. *fastidiosa* strain DSM 10026 (indicated hereafter as Xff) and *X. fastidiosa* subsp. *multiplex* strain DSM 103418 (Xfm) were supplied by DSMZ GmbH. The nucleic acids of *X. fastidiosa* subsp. *pauca* strain ST53 (Xfp) were kindly provided by the Phytosanitary Service of Lombardy region.

Nucleic acids from *P. syringae* strain 260-02 (indicated hereafter as 260-02) were extracted using GenElute™ Bacterial Genomic DNA Kit (Sigma-Aldich), following the manufacturer's instructions, as previously reported by Passera *et al.*, (2019).

After acquisition or extraction, all bacterial nucleic acids were stored at -30°C.

Nucleic acids from oleander (*Nerium oleander*) were extracted from asymptomatic whole leaf samples or midribs (0.5–1 g) using a CTAB method, described in EPPO standard 7/24 (EPPO, 2019). Oleander leaves were sampled in spring 2020 from three different asymptomatic plants, the samples were pooled together, and then kept frozen at -30°C until extraction in September 2020. Three samples of whole leaves were obtained and pooled together, while 4 samples of midribs only were obtained and assessed individually, as reported in the following paragraphs and Tables 1 and 2. Absence of *X. fastidiosa* in these samples was confirmed by including the nucleic acids from the plants, without spike of any kind, in all subsequent molecular assays: no amplification due to *X. fastidiosa* presence was detected in any of the nucleic acid samples extracted from asymptomatic *N. oleander* plants used in this study.

All quantifications of nucleic acids were carried out using a Nanodrop 1000 spectrophotometer.

Preparation of experimental samples and controls

Two sets of experimental samples and controls were prepared.

The first set was prepared by adding nucleic acids from oleander (using samples obtained from whole leaves, final concentration = 10 ng μL^{-1}) with nucleic acids from one of the three *X. fastidiosa* strains (final concentrations down to ten copies per µL, as shown in Table 1), or the 260-02 strain (final concentration = 10^5 copies per µL). The theoretical copy numbers of the bacterial genomes were estimated using concentration of the nucleic acids, the size of the genome, and the average molecular weight of a DNA base pair to calculate molarity, and, therefore, the number of molecules in the volume. Positive controls included nucleic acids from one of the three *X. fastidiosa* strains at different final concentrations, as shown in Table 1. Negative controls included nucleic acids either from the 260-02 strain, only from oleander, from oleander with 260-02 added, or no nucleic acids (NTC), as shown in Table 1.

The second set of samples and controls was prepared to further assess possible interference from the plant matrix in a sample more closely resembling those obtained during actual surveys for *X. fastidiosa* diagnoses. DNA was extracted from four samples each of 0.5 g of midribs from asymptomatic oleander plants. Each of the three Xf subspecies was added to each DNA sample at the following concentrations: Xff approx. 250 or 125 copies per µL, Xfm approx. 150 or 75 copies per µL, Xfp approx. 275 or 140 copies per µL, for a total of 6 experimental samples from each single starting DNA. DNA samples without added Xf DNA were also employed as negative controls in this experiment. All the samples and controls included in this second set are reported in Table 2.

Xylella fastidiosa *detection using qPCR*

The presence of Xf in the samples was determined using the SYBR Green assay (Francis *et al.*, 2006), and

Table 1. List of samples, positive controls, and negative controls included in the first set of analyzed material. The table reports for each sample/control the name, composition of host DNA and the source of added DNA. The concentration of the nucleic acids is expressed either as ng μL^{-1} or copy number per µL, depending on which parameter was more relevant during the preparation of the sample. This concentration value is an approximation used to express the order of magnitude of the target (for copies per µL) or rounded to the nearest multiple of 5 (for ng μL^{-1}).

Sample	Host DNA		Added DNA		Category
	Host	Concentration	Bacterium	Concentration	
OXFM_4	*N. oleander*	10 ng/µL	*X. fastidiosa* subsp. *multiplex*	10^4 copies/µL	Sample
OXFM_3	*N. oleander*	10 ng/µL	*X. fastidiosa* subsp. *multiplex*	10^3 copies/µL	Sample
OXFM_2	*N. oleander*	10 ng/µL	*X. fastidiosa* subsp. *multiplex*	10^2 copies/µL	Sample
OXFM_1	*N. oleander*	10 ng/µL	*X. fastidiosa* subsp. *multiplex*	10^1 copies/µL	Sample
OXFF_4	*N. oleander*	10 ng/µL	*X. fastidiosa* subsp. *fastidiosa*	10^4 copies/µL	Sample
OXFF_3	*N. oleander*	10 ng/µL	*X. fastidiosa* subsp. *fastidiosa*	10^3 copies/µL	Sample
OXFF_2	*N. oleander*	10 ng/µL	*X. fastidiosa* subsp. *fastidiosa*	10^2 copies/µL	Sample
OXFF_1	*N. oleander*	10 ng/µL	*X. fastidiosa* subsp. *fastidiosa*	10^1 copies/µL	Sample
OXFP_3	*N. oleander*	10 ng/µL	*X. fastidiosa* subsp. *pauca*	10^3 copies/µL	Sample
OXFP_2	*N. oleander*	10 ng/µL	*X. fastidiosa* subsp. *pauca*	10^2 copies/µL	Sample
OXFP_1	*N. oleander*	10 ng/µL	*X. fastidiosa* subsp. *pauca*	10^1 copies/µL	Sample
XFM-2	None	-	*X. fastidiosa* subsp. *multiplex*	0.5 ng/µL	Positive Control
XFM-3	None	-	*X. fastidiosa* subsp. *multiplex*	0.05 ng/µL	Positive Control
XFM-4	None	-	*X. fastidiosa* subsp. *multiplex*	0.005 ng/µL	Positive Control
XFM-5	None	-	*X. fastidiosa* subsp. *multiplex*	0.0005 ng/µL	Positive Control
XFF-2	None	-	*X. fastidiosa* subsp. *fastidiosa*	0.5 ng/µL	Positive Control
XFF-3	None	-	*X. fastidiosa* subsp. *fastidiosa*	0.05 ng/µL	Positive Control
XFF-4	None	-	*X. fastidiosa* subsp. *fastidiosa*	0.005 ng/µL	Positive Control
XFF-5	None	-	*X. fastidiosa* subsp. *fastidiosa*	0.0005 ng/µL	Positive Control
XFP-2	None	-	*X. fastidiosa* subsp. *pauca*	0.05 ng/µL	Positive Control
XFP-3	None	-	*X. fastidiosa* subsp. *pauca*	0.005 ng/µL	Positive Control
XFP-4	None	-	*X. fastidiosa* subsp. *pauca*	0.0005 ng/µL	Positive Control
XFP-5	None	-	*X. fastidiosa* subsp. *pauca*	0.00005 ng/µL	Positive Control
Oleander	*N. oleander*	10 ng/µL	None	-	Negative Control
OPSS_5	*N. oleander*	10 ng/µL	*P. syringae* strain 260-02	10^5 copies/µL	Negative Control
PSS	None	-	*P. syringae* strain 260-02	85 ng/µL	Negative Control
NTC	None	-	None	-	Negative Control

a TaqMan assay (Harper *et al.* (2010), erratum 2013). The methods for these two assays are outlined in EPPO standard PM 7/24 (EPPO, 2019).

The first method uses a pair of specific primers for XF, that was designed on the sequence of a conserved hypothetical protein gene: HL5 (5'-AAGGCAATAAACGCG-CACTA-3') and HL6 (5'-GGTTTTGCTGACTG-GCAACA-3'). This primer pair amplifies a segment of length 221 bp. The reaction mix was prepared as indicated in the EPPO standard PM 7/24 (4) (Francis *et al.*, 2006; EPPO, 2019), modified as follows: the volume of template nucleic acids was doubled and the total reaction volume was raised to 12 µL. The final composition of the mix was as follows: PowerSYBR master mix (Applied Biosystems) 1×, primer HL5 0.28 µM, primer HL6 0.28 µM, DNA template 2 µL, and water up to a volume of 12 µL.

The second method uses a specific primer pair which amplifies a sequence located in the *rimM* gene coding for a 16S rRNA processing protein: XF-F (5'-CACG-GCTGGTAACGGAAGA-3') and XF-R (5'-CACGGCTG-GTAACGGAAGA-3'), and the probe XF-P (5'-6-FAM-TCGCAT CCCGTGGCTCAGTCC-BHQ-1-3').

Each reaction mix was prepared as indicated in the EPPO standard PM 7/24 (Harper *et al.*, 2010; EPPO, 2019), modified as follows: the total reaction volume was reduced to 12 µL. The final composition of the mix was: TaqMan Universal Master Mix No Amperase (Applied Biosystems) 1×, primer XF-F 0.3 µM, primer XF-R 0.3 µM, probe XF-P 0.1 µM, BSA 0.3 µg μL^{-1}, DNA template 2 µL, and water up to volume of 12 µL.

For both methods, the changes in volumes of the reactions in comparison with that described in the

Table 2. List of samples, positive controls, and negative controls included in the second set of analyzed material. The table reports for each sample/control the name, composition of host DNA and the source of added DNA. The concentration of the nucleic acids is expressed as copy number per μL.

Sample	Host DNA		Added DNA		Category
	Host	Concentration	Bacterium	Concentration	
O1_XFM_2	*N. oleander*	418 ng/μL	*X. fastidiosa* subsp. *multiplex*	150 copies/μL	Sample
O1_XFM_1	*N. oleander*	418 ng/μL	*X. fastidiosa* subsp. *multiplex*	75 copies/μL	Sample
O1_XFF_2	*N. oleander*	418 ng/μL	*X. fastidiosa* subsp. *fastidiosa*	250 copies/μL	Sample
O1_XFF_1	*N. oleander*	418 ng/μL	*X. fastidiosa* subsp. *fastidiosa*	125 copies/μL	Sample
O1_XFP_2	*N. oleander*	418 ng/μL	*X. fastidiosa* subsp. *pauca*	275 copies/μL	Sample
O1_XFP_1	*N. oleander*	418 ng/μL	*X. fastidiosa* subsp. *pauca*	140 copies/μL	Sample
O1_C	*N. oleander*	418 ng/μL	None	-	Negative Control
O2_XFM_2	*N. oleander*	378 ng/μL	*X. fastidiosa* subsp. *multiplex*	150 copies/μL	Sample
O2_XFM_1	*N. oleander*	378 ng/μL	*X. fastidiosa* subsp. *multiplex*	75 copies/μL	Sample
O2_XFF_2	*N. oleander*	378 ng/μL	*X. fastidiosa* subsp. *fastidiosa*	250 copies/μL	Sample
O2_XFF_1	*N. oleander*	378 ng/μL	*X. fastidiosa* subsp. *fastidiosa*	125 copies/μL	Sample
O2_XFP_2	*N. oleander*	378 ng/μL	*X. fastidiosa* subsp. *pauca*	275 copies/μL	Sample
O2_XFP_1	*N. oleander*	378 ng/μL	*X. fastidiosa* subsp. *pauca*	140 copies/μL	Sample
O2_C	*N. oleander*	378 ng/μL	None	-	Negative Control
O3_XFM_2	*N. oleander*	316 ng/μL	*X. fastidiosa* subsp. *multiplex*	150 copies/μL	Sample
O3_XFM_1	*N. oleander*	316 ng/μL	*X. fastidiosa* subsp. *multiplex*	75 copies/μL	Sample
O3_XFF_2	*N. oleander*	316 ng/μL	*X. fastidiosa* subsp. *fastidiosa*	250 copies/μL	Sample
O3_XFF_1	*N. oleander*	316 ng/μL	*X. fastidiosa* subsp. *fastidiosa*	125 copies/μL	Sample
O3_XFP_2	*N. oleander*	316 ng/μL	*X. fastidiosa* subsp. *pauca*	275 copies/μL	Sample
O3_XFP_1	*N. oleander*	316 ng/μL	*X. fastidiosa* subsp. *pauca*	140 copies/μL	Sample
O3_C	*N. oleander*	316 ng/μL	None	-	Negative Control
O4_XFM_2	*N. oleander*	344 ng/μL	*X. fastidiosa* subsp. *multiplex*	150 copies/μL	Sample
O4_XFM_1	*N. oleander*	344 ng/μL	*X. fastidiosa* subsp. *multiplex*	75 copies/μL	Sample
O4_XFF_2	*N. oleander*	344 ng/μL	*X. fastidiosa* subsp. *fastidiosa*	250 copies/μL	Sample
O4_XFF_1	*N. oleander*	344 ng/μL	*X. fastidiosa* subsp. *fastidiosa*	125 copies/μL	Sample
O4_XFP_2	*N. oleander*	344 ng/μL	*X. fastidiosa* subsp. *pauca*	275 copies/μL	Sample
O4_XFP_1	*N. oleander*	344 ng/μL	*X. fastidiosa* subsp. *pauca*	140 copies/μL	Sample
O4_C	*N. oleander*	344 ng/μL	None	-	Negative Control
N_XFM_2	None	-	*X. fastidiosa* subsp. *multiplex*	150 copies/μL	Positive Control
N_XFM_1	None	-	*X. fastidiosa* subsp. *multiplex*	75 copies/μL	Positive Control
N_XFF_2	None	-	*X. fastidiosa* subsp. *fastidiosa*	250 copies/μL	Positive Control
N_XFF_1	None	-	*X. fastidiosa* subsp. *fastidiosa*	125 copies/μL	Positive Control
N_XFP_2	None	-	*X. fastidiosa* subsp. *pauca*	275 copies/μL	Positive Control
N_XFP_1	None	-	*X. fastidiosa* subsp. *pauca*	140 copies/μL	Positive Control
NTC	None	-	None	-	Negative Control

EPPO standard (EPPO, 2019) were carried out to be more similar to the operative conditions of the dPCR assay, which uses a total volume of 12 μL, as reported in the handbook for the reaction mixes. Using the same total reaction and experimental sample volumes assures that the concentration of target DNA is the same in both assays, making the results directly comparable.

These reactions were carried out in StepOnePlus Real-Time PCR thermocycler (Thermo Fisher Scientific). The thermal cycling profile used for both methods was as described in the EPPO standard (EPPO, 2019).

All the samples reported in Table 1 were tested with both methods. Each sample and control were analysed in triplicate.

For assessing the results obtained, in accordance with two methods described in the EPPO standard (EPPO, 2019), the quantification cycle (Cq) was evaluated for both the Taqman and SYBR Green methods,

and the melting temperature (Tm) was evaluated for the SYBR Green method.

Xylella fastidiosa *detection and quantification using dPCR*

The presence and quantity of XF in the samples and controls were assessed in nanoplate-based dPCR, using the QIAcuity instrument (Qiagen). The results obtained were analyzed using the QIAcuity Software Suite version 2.0.20.

The methods of Francis *et al.* (2006) and Harper *et al.* (2010) were carried out in dPCR. The reaction mixes were set up with the same composition as the corresponding mixes used for the qPCR assays, but using the EG PCR Master Mix 3× (Qiagen) in place of the PowerSYBR mix, and QIAcuity Probe PCR Master Mix 4× (Qiagen) in place of TaqMan Universal Master Mix No Amperase. Both master mixes were used at final concentrations of 1×.

To keep these reactions as close as possible to the original methods used in qPCR, no restriction enzyme was added to the mixes, although use of a restriction enzyme is normally suggested in instructions for the master mixes used in dPCR.

The reactions were carried out in 96 well QIAcuity Nanoplates, with 8.5K partitions per well. All the samples and controls reported in Table 1 were assayed with both methods. Each sample and control were tested in duplicate. All the samples and controls reported in Table 2 were assayed with both methods, without carrying out technical replicates, with the exception of NTC, which was assayed in triplicate.

For the Eva Green (EG) protocol, thermal cycling was as follows: one cycle of incubation at 95°C for 2 min; 40 cycles of 95°C for 15 sec, 60°C for 15 sec, and 72°C for 15 sec; then incubation at 40°C for 5 min. This cycle followed instructions in the EG PCR Master Mix 3× (Qiagen) handbook, changing only the annealing temperatures to match that of the primers employed. Imaging was carried out with 700 ms of exposure and a gain value of 8.

For the Probe protocol, thermal cycling was as follows: one cycle of incubation at 95°C for 2 min; 40 cycles of 95°C for 15 sec, and 62°C for 30 sec. This followed the instructions of the Probe PCR Master Mix 4× (Qiagen) handbook, changing only the annealing temperature to match that for the primers employed. Imaging was carried out with 500 ms of exposure and a gain value of 6.

Evaluation of diagnostic performance parameters

For each test, parameters were calculated as follows:
Accuracy = 100 × (PA + NA) / (PA + NA + PD + FD);
Sensitivity = 100 × PA / (PA + ND);
Specificity = 100 × NA / (NA + PD);
where PA was positive agreement (a positive result is obtained when a positive result is expected), NA is negative agreement (a negative result is obtained when a negative result is expected), PD is positive deviation (a positive result is obtained when a negative result is expected), and ND is negative deviation (a negative result is obtained when a positive result is expected).

RESULTS

Xylella fastidiosa *detection through qPCR*

The qPCR assays correctly detected the presence of Xff, Xfm and Xfp in all the experimental samples and positive controls (Table 1, Figure 1), regardless of the primer pairs employed. For all samples and positive controls, the qPCR assays yielded the expected results, with Cq increasing as the concentration of pathogen decreased and, for the SYBR Green assay, giving a single, recognizable Tm peak for each sample. The assays therefore detected the pathogen at an order of magnitude as low as ten copies per µL.

The TaqMan assay gave an expected result of "undetected" for all the negative controls. On the other hand, the SYBR Green assay gave as result a Cq also on negative samples and controls. The NTC gave an average Cq of 37.32, which is indicated as an undetermined result, but did not show exponential amplification nor the correct Tm of the amplicon and are therefore considered as negative results as indicated in the protocol (EPPO, 2019). However, other negative controls gave results that could be mistaken as positive based on Cq alone. These included *N. oleander* with added *P. syringae* nucleic acids (OPSS_5), or without these nucleic acids (Oleander), gave Cq values between 32 and 34, regardless of the presence of added nucleic acids, while nucleic acids from *P. syringae* pure culture (PSS) gave an average Cq of 33.82. Analysis of the melting curves showed that these results were due to non-specific amplification: Tm was consistent between samples with added Xf subspecies (average 83.15°C), while in the samples without Xf DNA the Tm varied between 61–93°C, without clear, defined peaks in the melting curves.

Xylella fastidiosa *detection through dPCR*

Results of dPCR assays from the Eva Green (EG) and the Probe methods for each control and sample reported in Table 1 indicated that both primer pairs

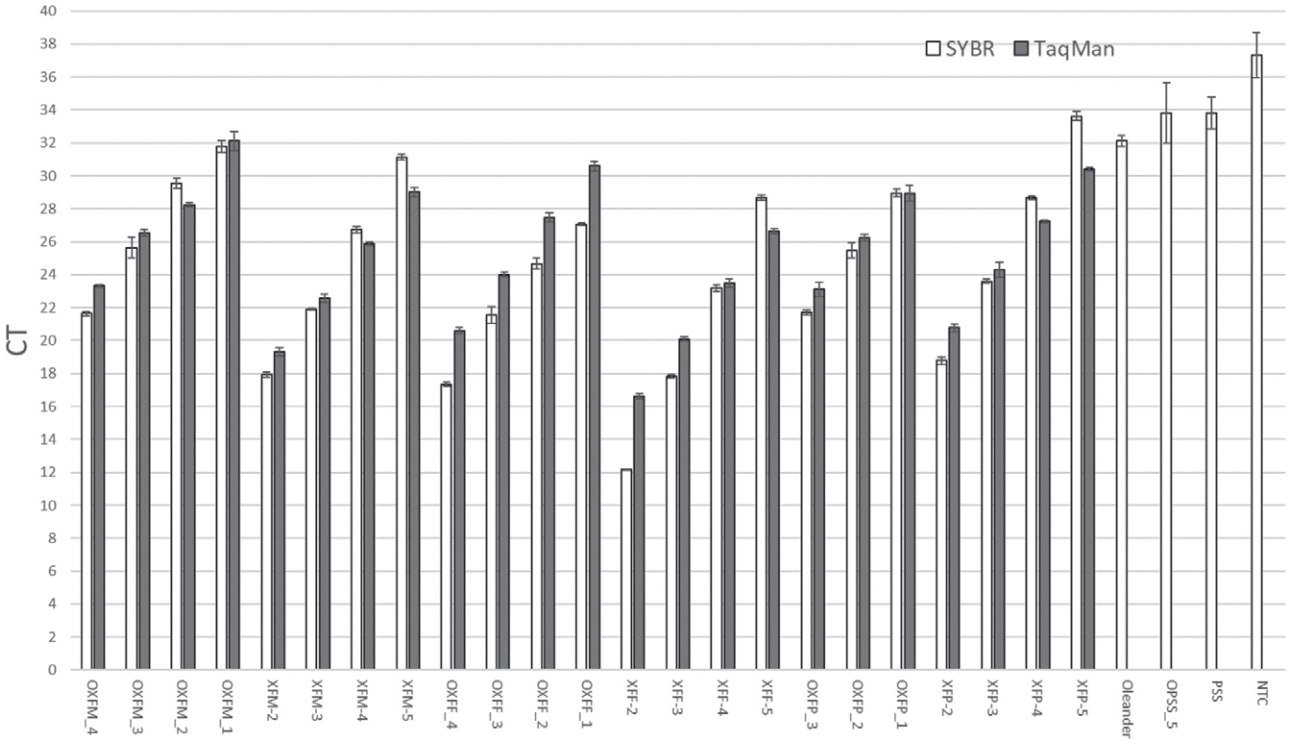

Figure 1. Results from qPCR *Xylella fastidiosa* detection assays. The graph shows different samples (Table 1) on the X-axis, and quantification cycles (Cq) obtained on the Y-axis. For each sample, the grey bars are results of TaqMan assays (Harper *et al.*, 2010) while the white bars are results of the SYBR Green assay (Francis *et al.*, 2006). The represented number for each Cq is the average obtained from three replicates, and the error bar represents the standard deviation. Where no bar is present, the result of the assay was "undetected".

amplified as intended. Some examples of the outputs produced by the dPCR are presented in Supplementary Figures 1 and 2.

For the EG method, a strong background fluorescence was detected, with a fluorescence for negative partitions ranging from 50 to 135 RFU, while the positive partitions had intensity of 200 to 250 RFU (Figure 2A). It is important to note that the RFUs for negative controls are different between the NTC or *P. syringae* DNA, and those that contain DNA of *N. oleander*, being greater for *N. oleander* DNA. This could be due to some non-specific annealing of the primers producing some DNA amplicons, in line with the results obtained with qPCR. Also, there is likely presence of some 'rain' in the samples and positive controls, defined as partitions that give intermediate fluorescence between negative and positive (in this case 135-200 RFU), which were found with high frequency in the XFM samples and controls. To determine the effect of the threshold level on detection and quantification of XF, results include two different thresholds. The first threshold was set just above the RFU of the negative cloud (dMIQE group, 2020) which is presented under the code EG_135, since the threshold is at 135 RFU. The second threshold was set at the lowest border of the positive cloud, effectively removing the 'rain' partitions, which is presented under the code of EG_200, since the threshold is set at 200 RFU (Table 3). The Probe method showed an overall lower level of fluorescence, both for negative and positive partitions: negative partitions had fluorescence of 10 to 20 RFU, while the positive partitions ranged from approx. 40 to 60 RFU (Figure 2B). This result is in line with the lower exposition time and gain utilized for the imaging. Although less common than in the EG method, also in this assay there was some 'rain', with fluorescence between 20 and 40 RFU. In order to determine the effects of the threshold level on detection and quantification of XF, results include two different thresholds: one set just above the RFU of the negative cloud (dMIQE group, 2020) which is presented under the code of Probe_20, since the threshold is at 20 RFU; the second threshold was set at the lowest border of the positive cloud, effectively removing the 'rain' partitions, which is presented under the code of Probe_40, since the threshold is set at 40 RFU (Table 3).

Detection and quantification of the pathogen was possible in all samples and positive controls (Table 3),

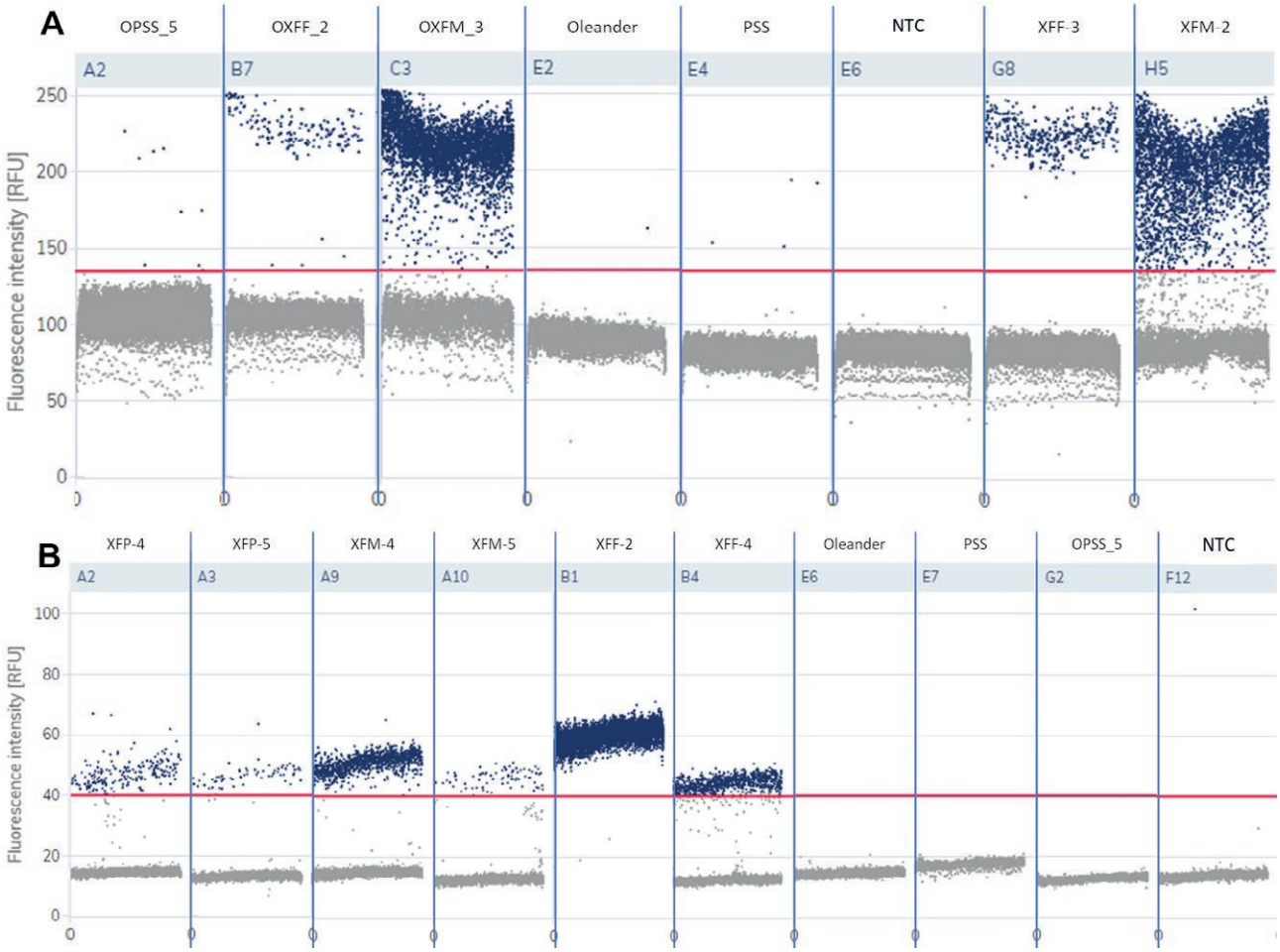

Figure 2. 1-D Scatterplots of representative samples for dPCR assays. Each box represents the fluorescence value (expressed as RFU) for each partition, the red line shows the threshold. Each partition above the threshold (in blue) is considered positive, while each below the threshold (in grey) is considered negative. A) Representative samples for the EG method, with threshold set at 135 RFU. This same dataset was also analysed with the threshold set at 200 RFU. B) Representative samples for the Probe method, with threshold set at 40 RFU. This same dataset was also analysed with the threshold set at 20 RFU.

regardless of the threshold setting, for both the EG and Probe methods. Taking into consideration that there was no standardized protocol to follow for these methods for nanoplate-based dPCR, and that the present study was carried out only on experimental samples and controls of known status (positive and negative), also certified by two different qPCR diagnostic methods, the parameters to discriminate between positive or negative results were not decided beforehand, but were instead formulated by analyzing the present results. For copy numbers of targets per µL and confidence intervals, it was possible to discriminate between positive and negative results by setting threshold copy number for a positive result as greater than the average target copy number detected in negative controls, taking into consideration the greatest bounds of the confidence intervals. Due to the rare cases of amplification in the negative controls, this threshold was calculated as 12 for EG_135, 2 for EG_200, 3 for Probe_20, and 2 for Probe_40 (Table 3). The numbers of copies to consider a sample positive were greater in the cases of lower thresholds (EG_135 and Probe_20), as there was presence of 'rain' partitions in the negative controls, but there was negligible influence of the threshold setting in the Probe method. Also when considering 'rain' partitions as positive, in line with dMIQE guidelines, in no case was there a copy number of target sequence greater than 10 for negative controls, or less than 10 for samples and positive controls (Table 3). Nevertheless, considering that ten target copies is close to the greatest registered also for negative controls, an order of magnitude of ten copies of target per µL of sample was the limit of detection for these assays.

Table 3. Results of dPCR assays on the first set of samples, positive and negative controls. The table reports the target copy number/μL for each sample, the error is calculated as a CI of 95%. The columns report the results obtained with either the EG or Probe method with the two considered thresholds. Copy number was rounded to the closest unit. The error is rounded to the closest decimal.

Sample	Digital PCR results (copies/μL of template)			
	EG (Francis *et al.*, 2006)		Probe (Harper *et al.*, 2010)	
	EG_135	EG_200	Probe_20	Probe_40
OXFM_4	16,469 ± 2.1%	13,404 ± 2.6%	14,783 ± 2.2%	13,254 ± 2.6%
OXFM_3	1,602 ± 7.2%	1,303 ± 7.9%	1,730 ± 7.7%	1,556 ± 7.9%
OXFM_2	152 ± 23.6%	133 ± 25.1%	158 ± 25.9%	148 ± 26.1%
OXFM_1	24 ± 61.5%	19 ± 67.5%	13 ± 94.5%	10 ± 95.2%
OXFF_4	22,420 ± 2.2%	22,419 ± 2.1%	19,815 ± 2.1%	17,830 ± 2.2%
OXFF_3	2,215 ± 6.1%	2,188 ± 6.1%	2,756 ± 6.0%	2,437 ± 6.0%
OXFF_2	306 ± 16.5%	294 ± 16.9%	279 ± 19.3%	242 ± 19.7%
OXFF_1	17 ± 73.3%	16 ± 75.6%	16 ± 84.6%	14 ± 84.5%
OXFP_3	5,054 ± 4.2%	5,025 ± 4.2%	4,556 ± 4.6%	4,096 ± 4.6%
OXFP_2	600 ± 12.6%	579 ± 12.9%	585 ± 13.1%	525 ± 13.1%
OXFP_1	84 ± 33.7%	81 ± 34.0%	81 ± 36.4%	72 ± 36.5%
XFM-2	N/A (oversaturated)	N/A (oversaturated)	N/A (oversaturated)	N/A (oversaturated)
XFM-3	88,351 ± 0.7%	67,076 ± 1.0%	26,173 ± 1.9%	24,891 ± 1.9%
XFM-4	8,370 ± 3.2%	4,285 ± 4.9%	2,682 ± 5.6%	2,656 ± 5.6%
XFM-5	955 ± 8.2%	427 ± 14.5%	208 ± 24.2%	161 ± 24.7%
XFF-2	N/A (oversaturated)	N/A (oversaturated)	N/A (oversaturated)	N/A (oversaturated)
XFF-3	41,228 ± 1.8%	41,226 ± 1.8%	33,491 ± 1.9%	30,160 ± 1.60%
XFF-4	2,272 ± 6.6%	2,189 ± 6.6%	2,266 ± 6.2%	2,039 ± 6.6%
XFF-5	152 ± 24.2%	150 ± 24.3%	145 ± 26.7%	123 ± 27.8%
XFP-2	13,429 ± 2.2%	13,428 ± 2.2%	12,377 ± 1.6%	11,152 ± 2.7%
XFP-3	2,015 ± 6.8%	2,012 ± 6.8%	1,648 ± 7.61%	1,465 ± 7.9%
XFP-4	184 ± 23.9%	181 ± 24.0%	162 ± 25.7%	142 ± 26.0%
XFP-5	35 ± 57.9%	32 ± 58.7%	29 ± 61.9%	25 ± 63.8%
Oleander	3 ± 274.4%	0	0	0
OPSS_5	3 ± 171.6%	1 ± 109.1%	0	0
PSS	8 ± 138.8%	0	0	0
NTC	0	0	1 ± 275.4%	1 ± 168.6%
Threshold	>12	>2	>3	>2

The results obtained with both assays confirmed the theoretical concentration of Xf in the experimental samples and positive controls, as the concentration of target was always in the expected order of magnitude. The positive controls with the greatest concentrations of target, namely XFM-2 and XFF-2, caused the respective wells to be oversaturated. This result, while positive, did not allow quantification of the target concentrations, so was not optimal. While the order of magnitude of target copy number in the samples and positive controls was confirmed by the two different assays, there were differences in the results. samples and positive controls containing Xfm gave much greater copy numbers per μL when tested with the EG method than with the Probe method. This result is partially explained by the high number of 'rain' partitions in the Xfm samples tested with the EG dPCR method. The overestimation in this sample type was exemplified by the XFM-3 positive control. The Probe_20 and Probe_40 results were similar, with, respectively, 26,173 and 24,891 copies per μL. In contrast the results for EG_135 were 88,351 copies per μL, and 67,076 for EG_200. While the higher threshold caused overestimation of the target's quantity by 2.7 times, the lower threshold raised this error further to around 3.5

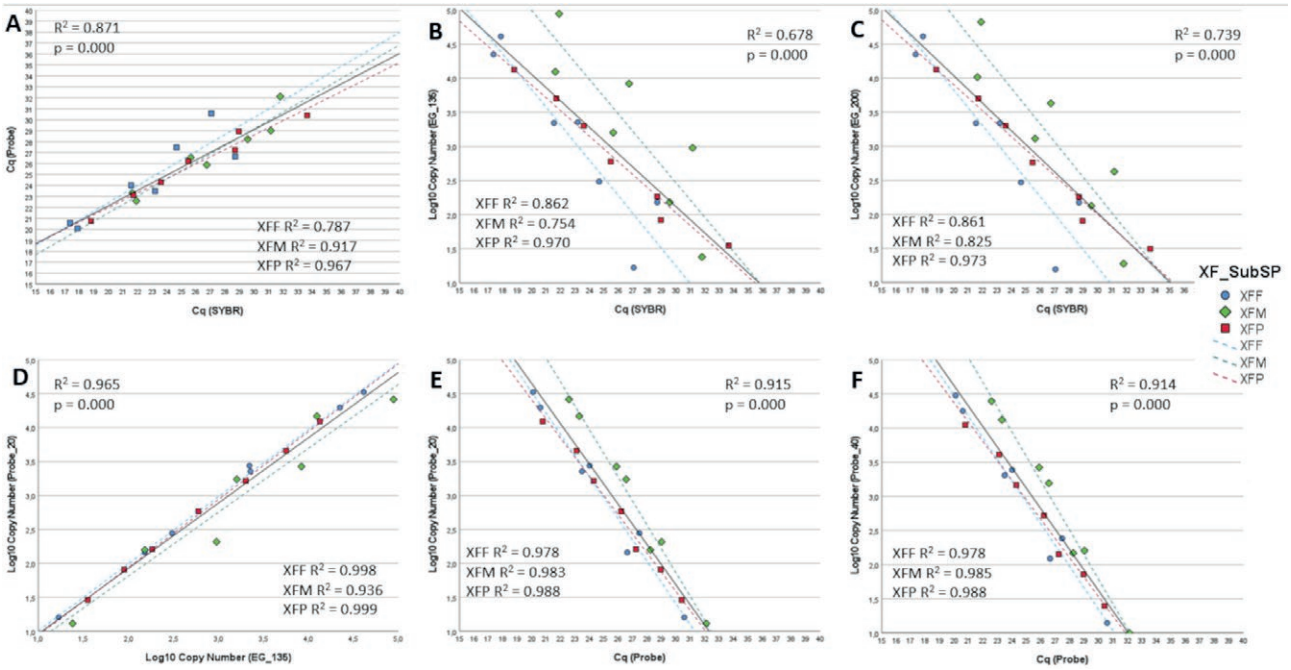

Figure 3. Scatterplots showing the correlations between results obtained by different diagnostic assays in the following pairs: (A) qPCR with SYBR Green on the X-axis and qPCR with Probe on the Y-axis; (B) qPCR with SYBR Green on the X-axis and dPCR with EG, threshold set at 135 RFU, on the Y-axis; (C) qPCR with SYBR Green on the X-axis and dPCR with EG, threshold set at 200 RFU, on the Y-axis; (D) dPCR with EG, threshold set at 135 RFU, on the X-axis and dPCR with Probe, threshold set at 20 RFU, on the Y-axis; (E) qPCR with Probe on the X-axis and dPCR with Probe, threshold set at 20 RFU, on the Y-axis; and (F) qPCR with Probe on the X-axis and dPCR with Probe, threshold set at 40 RFU, on the Y-axis. Markers on the plots indicate single samples, and their colours and shapes indicate the subspecies of *Xylella fastidiosa* they belong to, as reported in the legend. Each graph contains three dashed trendlines, which are calculated on samples belonging to a single subspecies, and a solid-line trendline, calculated on all the samples for each combination of the diagnostic assays. Each graph also reports the overall R^2 value and the *P* value obtained from linear regression analysis, as well as the R^2 value for each *X. fastidiosa* subspecies.

times greater. The positive control XFM-4 gave a similar result, with EG_200 giving a result two times greater than that obtained with the Probe method, and with EG_135 giving a result four times greater. For the samples and positive controls containing Xff and Xfp, these differences were not as pronounced, especially when the copy number was at 10^3 or less. While this overestimation of the target abundance for XFM did not interfere with detection of the pathogen, it would become an issue when accurate quantification is necessary.

Comparison between different diagnostic methods

All four methods employed in the study (qPCR SYBR Green, qPCR Probe, dPCR EG, dPCR Probe) detected presence of the target pathogens in the samples and positive controls, and did not detect the target pathogens in the negative controls. Having detected no differences between the expected results and experimental results, all four methods showed a 100% accuracy, diagnostic sensitivity, and specificity. All the methods also detected *X. fastidiosa* at all the tested concentrations, down to an order of magnitude of ten target copies per µL.

Since both the qPCR and dPCR approaches are quantitative, a direct comparison of the results obtained by the methods is possible. Linear regression analyses showed, that there was strong statistical significance ($P = 0.000$) for the correlations between results from the different diagnostic assays (Figure 3). Correlations for the different methods were especially high when comparing the two dPCR methods (Figure 3D), and the qPCR and dPCR using probes (Figures 3E and 4F), and with overall R^2 values greater than 0.9 and close to 1 when considering the individual Xf subspecies. The least correlations were measured for the comparisons between the qPCR with SYBR Green, and the dPCR with EG and threshold of 135 (Figure 3B). This was due to two distinct forms of bias that have been highlighted by the comparison of distinct methods. Firstly, Cq registered for Xff using the SYBR Green method was slightly less than those for the other two subspecies at equal concentrations of target. Secondly, the dPCR quantification for

Table 4. Results of dPCR assays on the second set of samples, positive and negative controls. The table reports the target copy number/μL for each sample, the error is calculated as a CI of 95%. The columns report the results obtained with either the Probe method with the two considered thresholds, or with EG with threshold at 200. Copy number was rounded to the closest unit. The error is rounded to the closest decimal.

Sample	Digital PCR results (copies/μL of template)		
	EG_200	Probe_20	Probe_40
O1_XFM_2	N/A (Oversaturated)	142 ± 26.9%	145 ± 26.6%
O1_XFM_1	N/A (Oversaturated)	79 ± 34.0%	76 ± 34.6%
O1_XFF_2	N/A (Oversaturated)	303 ± 17.3%	299 ± 17.5%
O1_XFF_1	N/A (Oversaturated)	129 ± 25.3%	125 ± 26.1%
O1_XFP_2	N/A (Oversaturated)	352 ± 16.1%	343 ± 16.3%
O1_XFP_1	N/A (Oversaturated)	154 ± 23.8%	152 ± 23.9%
O1_C	N/A (Oversaturated)	0	0
O2_XFM_2	N/A (Oversaturated)	120 ± 27.4%	120 ± 27.4%
O2_XFM_1	N/A (Oversaturated)	75 ± 38.3%	72 ± 39.1%
O2_XFF_2	N/A (Oversaturated)	258 ± 17.9%	251 ± 18.1%
O2_XFF_1	N/A (Oversaturated)	119 ± 27.1%	115 ± 27.9%
O2_XFP_2	N/A (Oversaturated)	275 ± 17.8%	269 ± 18.0%
O2_XFP_1	N/A (Oversaturated)	139 ± 25.7%	136 ± 25.8%
O2_C	N/A (Oversaturated)	0	0
O3_XFM_2	N/A (Oversaturated)	114 ± 27.9%	114 ± 27.9%
O3_XFM_1	N/A (Oversaturated)	97 ± 30.9%	90 ± 32.2%
O3_XFF_2	N/A (Oversaturated)	170 ± 22.0%	166 ± 22.3%
O3_XFF_1	N/A (Oversaturated)	130 ± 25.7%	123 ± 26.4%
O3_XFP_2	N/A (Oversaturated)	195 ± 21.5%	188 ± 21.3%
O3_XFP_1	N/A (Oversaturated)	102 ± 33.1%	138 ± 25.7%
O3_C	N/A (Oversaturated)	3 ± 274.0%	0
O4_XFM_2	N/A (Oversaturated)	142 ± 26.9%	144 ± 26.1%
O4_XFM_1	N/A (Oversaturated)	74 ± 38.7%	74 ± 38.7%
O4_XFF_2	N/A (Oversaturated)	266 ± 17.4%	254 ± 17.8%
O4_XFF_1	N/A (Oversaturated)	89 ± 30.5%	89 ± 30.5%
O4_XFP_2	N/A (Oversaturated)	188 ± 21.3%	188 ± 21.3%
O4_XFP_1	N/A (Oversaturated)	137 ± 25.9%	138 ± 25.7%
O4_C	N/A (Oversaturated)	0	0
N_XFM_2	13 ± 86.2%	120 ± 26.9%	117 ± 27.1%
N_XFM_1	2 ± 274.4%	65 ± 38.3%	65 ± 38.3%
N_XFF_2	174 ± 21.5%	278 ± 18.1%	262 ± 18.6%
N_XFF_1	124 ± 25.9%	121 ± 26.9%	118 ± 27.1%
N_XFP_2	366 ± 15.1%	323 ± 16.1%	323 ± 16.1%
N_XFP_1	20 ± 68.7%	150 ± 24.1%	148 ± 24.2%
NTC	2 ± 274.4%	1 ± 274%	0

Xfm gave greater copy number per μL than expected, mostly due to presence of many 'rain' partitions. These two effects reduced the R^2 values for the subspecies in which they were identified by small amounts (to 0.862 for Xff and 0.754 for Xfm). Overall, when both effects are considered together by evaluating all three Xf subspecies at the same time, they caused high reductions in correlations between the two methods, with an R^2 value of 0.678. The same analysis with the threshold at 200, ignoring the effect of the 'rain' partitions on Xfm, gave greater correlation with the qPCR results, with an R^2 values of 0.861 for Xff and 0.826 for Xfm, and an overall correlation of 0.739 (Figure 3C). Xfp gave consistently greater correlation values compared to other Xf subspecies, regardless of which two methods were being compared. A list of all R^2 values for the correlations of each pair of methods is presented in Supplementary Table 1.

Evaluation of plant matrix effect on detection through dPCR

The methods previously described and tested on samples that contained *N. oleander* DNA diluted to 10 ng μL^{-1} were tested on a set of samples and controls that resembled real samples that could be obtained by DNA extraction from infected host material. Results of dPCR EG and dPCR Probe from this set of samples and controls are shown in Table 4.

dPCR EG failed to provide useful information for this set of samples. The positive controls that contained only Xf were correctly amplified, but all samples and negative controls that contained undiluted *N. oleander* DNA resulted in oversaturation, probably caused by the high quantity of DNA that can bind to the non-specific EvaGreen reporter.

In contrast, the dPCR Probe method correctly detected the presence of Xf subspecies in all samples and positive controls, while giving negative results for the negative controls. The negative control O3_C with the threshold set at 20 had a total of three copies per μL. However, as the positive threshold was determined to be more than three for the Probe_20 method, it was still considered negative. With the threshold set at 40, all negative controls returned a concentration of zero copies of the targets.

Quantification of the pathogen concentrations was adequate with the dPCR Probe method, as the results were in line with the expected orders of magnitude for each sample and control.

DISCUSSION

Digital PCR (dPCR) is a technique that is recently being adopted in research laboratories and will probably not rapidly become widespread for diagnostic applications. Nevertheless, its potential benefits for detection and quantification of pathogens are many, and rapid

integration of this molecular technique in diagnostics could prove beneficial for early detections of pathogens, particularly for quarantine pests. Several examples of the use of dPCR as diagnostic tools are available in human medicine (Sedlak *et al.*, 2014; Mangolini *et al.*, 2015; Devonshire *et al.*, 2016), indicating the benefits that can be obtained from the use of this technique. While it is still a budding technology in plant health, there are some studies that have showed adaptation of qPCR assays to dPCR (Dreo *et al.*, 2014; Lu *et al.*, 2019; Maheshwari *et al.*, 2017; Zhao *et al.*, 2016; Dupas *et al.*, 2019). These studies utilized the droplet-based dPCR technology, which uses oil emulsions to create partitions as small droplets, which then each undergo amplification and analysis. This technology needs additional steps in adaptation of qPCR protocols, due to different working environments caused by the use of oil, and the available systems for droplet-based dPCR suffer from lower throughput compared to qPCR while requiring more steps for sample preparation (Dupas *et al.*, 2019). The system used in the present study was a nanoplate-based dPCR, which obtained the partition of the reaction mixture through the physical conformation of the reaction plate. This allowed direct adaptation of qPCR protocols, and could process a high number of samples at once.

The present study used qPCR and dPCR which gave comparable results for detection of *X. fastidiosa.* Both approaches showed high performance criteria, with accuracy, specificity, and diagnostic sensitivity equal to 100% in the first set of experimental samples. While some differences based on the pathogen subspecies were highlighted in these analyses, all the methods detected the pathogen, regardless of subspecies. All the results confirmed that dPCR and qPCR had similar performance criteria for detection of Xf, which was in accordance with a previous reported by Dupas *et al.* (2019). That study compared the qPCR diagnostic method of by Harper *et al.* (2010) for Xf with droplet-based dPCR. Both methods were effective for detection of the pathogen, and there was high correlation between copy numbers detected by droplet-based dPCR and the Cq values from qPCR. Since it is reported that the benefits obtained from the use of dPCR can be dependent on the studied pathosystem (Dreo *et al.*, 2014), it is significant that the present results confirm that dPCR can be suitable for the detection of Xf, using different plant matrices and dPCR technology than those tested by Dupas *et al.* (2019). Quantification of Xf through dPCR was an improvement compared with qPCR, which would result in increased throughput in the pathogen diagnoses. Since qPCR can only achieve relative quantifications in comparison to reference material, using this technique to quantify target copy numbers requires the inclusion of standards with known concentrations, which uses up several wells in each assay plate. Obtaining accurate, absolute pathogen quantification without using such standards allows the processing of large numbers of samples per reaction. Such standards may not always be available. For Xf, axenic culturing is possible, so standards of known quantity can be developed to make absolute quantifications through qPCR. This is not the case for many other plant pathogens, for which the use of dPCR for quantitative assays offers benefit (Gutierrez-Aguire *et al.*, 2015). Considering that standard qPCR procedures analyze two or three replicates for each sample, use of dPCR, with results from thousands of repetitions in each well, can increase the numbers of samples processed per reaction, removing the limitation of employing several wells per sample. The increase of throughput can translate into shortening of the technical time needed to carry out diagnoses for many samples and also in reduced per sample analysis costs.

As dPCR is a quantitative and highly sensitive assay, it rarely gives exclusively negative results (zero positive partitions), and could also show some partitions with fluorescence from negative samples, in a way similar to how qPCR can give late Cq values greater than 37 for negative samples. Therefore, it is necessary to set thresholds to discriminate between positive and negative results, especially for EG methods that do not use specific probes. In the present analyses, setting the threshold at the highest copy number per µL detected in a known negative control (adjusted to the highest range of the confidence interval) allowed discrimination between positive and negative samples. This result will need further confirmation and validation before it can be used as a threshold for true diagnostic tests, especially considering that for EG_135 the threshold was high, at 12 copies per µL and could theoretically cause positive samples with ten copies per µL to be incorrectly classified as negatives. Also, the possibility of adding more negative and non-template controls to each plate could be considered, to more precisely estimate how many positive partitions are detected in negative samples when working with environmental samples.

In conclusion, EG and Probe dPCR methods, with either low thresholds set just above the cloud of negative partitions or higher thresholds set just below the cloud of positive partitions, were able to detect the presence of three different Xf subspecies in the analyzed samples. For the quantification, the EG method was not reliable for Xfm, and, especially with the lower threshold (EG_135), it detected several positive partitions in negative controls. Concern regarding fluorescence derived from non-specific amplification was more relevant in EG

dPCR. as, compared to SYBR Green assays carried out on qPCR, the lack of a melting curve step might contribute to incorrect positive detections in samples that do not contain the targets organisms. This concern was a major downfall of the method for the second set of samples containing large quantities of non-target DNA, in line with what would be obtained from extractions from infected plant material. This caused oversaturation of the wells even in the negative controls. Also, this method showed relevant production of 'rain', in particular for Xfm, that could contribute to uncertainty in the data analyses. In contrast, having lower values for positive partitions in the negative controls, guaranteed by using specific primers and a specific probe, the present study results suggest that using the protocol described by Harper *et al.* (2010) could give more reliable results. These considerations, in particular the completely unreliable results obtained when using samples that contained 300-600 ng per µL of host plant DNA, suggest that the EG method should not be employed for actual diagnostics, while the Probe dPCR method was reliable.

This study indicates the potential benefits of using nanoplate-based dPCR as a technique that can substitute traditional qPCR assays for detection of Xf, offering comparable performance criteria and the possibility of increased sample throughput, lowering the time and cost of analyses. This study is a first step demonstrating the possibility of using this technique for diagnostic applications in plant pathology. Before being utilized in actual diagnoses, these results should be validated by accredited laboratories, using more samples and including naturally infected plants.

ACKNOWLEDGMENTS

The authors gratefully acknowledge Vivai Nord s.n.c. for providing *Nerium oleander* plant tissues, and Bachelor Student Anna Leone for the support with DNA extraction and preparation of experiment reactions. The Department of Agricultural and Environmental Sciences of the University of Milan, with the REE initiative, allowed acquisition of the digital PCR instrument used in this study. This research was funded by Regione Lombardia, GARDING project (prot. dom. M1.2018.0067306).

DATA AVAILABILITY STATEMENT

All relevant data are within the paper and its Supporting Information files.

LITERATURE CITED

Backus E.A., Morgan D.J.W., 2011. Spatiotemporal colonization of *Xylella fastidiosa* in its vector supports the role of egestion in the inoculation mechanism of foregut-borne plant pathogens. *Phytopathology* 101: 869–884.

Baldi P., La Porta N., 2017. *Xylella fastidiosa*: host range and advance in molecular identification techniques. *Frontiers in Plant Sciences* 8: 944. DOI: 10.3389/fpls.2017.00944

Chang C.J., Garnier M., Zreik L., Rossetti V., Bové J.M., 1993. Culture and serological detection of the xylem-limited bacterium causing citrus variegated chlorosis and its identification as a strain of *Xylella fastidiosa*. *Current Microbiology* 27: 137–142. DOI: 10.1007/BF01576010

Cornara D., Sicard A., Zeilinger A.R., Porcelli F., Purcell A.H., Almeida R.P.P., 2016. Transmission of *Xylella fastidiosa* to grapevine by the meadow spittlebug. *Phytopathology* 106: 1285–1290.

Davis M.J., Purcell A.H., Thomson S.V., 1978. Pierce's disease of grapevines: isolation of the causal bacterium. *Science* 199: 75–77. DOI: 10.1126/science.199.4324.75

Desprez-Loustau M.L., Balci Y., Cornara D., Gonthier P., Robin C., Jacques M.A., 2020. Is Xylella fastidiosa a serious threat to European forests? *Forestry* 94: 1–17. DOI: 10.1093/forestry/cpaa029

Devonshire A.S., O'Sullivan D.M., Honeyborne I., Jones G., Karczmarczyk M., (…), Huggett J.F., 2016. The use of digital PCR to improve the application of quantitative molecular diagnostic methods for tuberculosis. *BMC Infectious Diseases* 16: 366. DOI: 10.1186/s12879-016-1696-7

dMIQE group, 2020. The Digital MIQE guidelines update: minimum information for publication of quantitative digital PCR experiments for 2020. *Clinical Chemistry* 66: 1012–1029. DOI: 10.1093/clinchem/hvaa125

Dreo T., Pirc M., Ramsak Z., Pavsic J., Milavec M., Zel J., Gruden K., 2014. Optimising droplet digital PCR analysis approaches for detection and quantification of bacteria: a case study of fire blight and potato brown rot. *Analytical and Bioanalytical Chemistry* 406: 6512–6528. DOI: 10.1007/s00216-014-8084-1

Dupas E., Legendre B., Olivier V., Poliakoff F., Manceau C., Cunty A., 2019. Comparison of real-time PCR and droplet digital PCR for the detection of Xylella fastidiosa in plants. *Journal of Microbiological Methods* 162: 86–95. DOI: 10.1016/j.mimet.2019.05.010

EFSA (European Food Security Authority), 2022. Update of the *Xylella* spp. host plant database–systematic lit-

erature search up to 30 June 2021. 12 January 2022. *EFSA Journal* 20: 7039. DOI: 10.2903/j.efsa.2022.7039

Faino L., Scala V., Albanese A., Modesti V., Grottoli A., (…), Loreti S., 2021. Nanopore sequencing for the detection and identification of *Xylella fastidiosa* subspecies and sequence types from naturally infected plant material. *Plant Pathology* 70: 1860–1870. DOI: 10.1111/ppa.13416

Francis M., Lin H., Cabrera-La Rosa J., Doddapaneni H., Civerolo E.L., 2006. Genome-based PCR primers for specific and sensitive detection and quantification of *Xylella fastidiosa*. *European Journal of Plant Pathology* 115: 203–213.

Frazier N.W., 1965. Xylem viruses and their insect vectors. In: *Proceeding of the International Conference of Virus Vectors Perennial Hosts Special Ref. Vitis*. Ed. WB Hewitt, pages 91-99. Davis, CA: Division of Agricultural Science, University of California.

Gutierrez-Aguirre I., Racki N., Dreo T., Ravniakr M., 2015. Droplet digital PCR for absolute quantification of pathogens. *Methods in Molecular Biology* 1302: 331–347. DOI: 10.1007/978-1-4939-2620-6_24

Harper S.J., Ward, L.I. Clover G.R.G., 2010. Development of LAMP and real-time PCR methods for the rapid detection of *Xylella fastidiosa* for quarantine and field applications. *Phytopathology* 100: 1282–1288.

Lu Y., Zhang H., Wen C., Wu P., Song S., (…), Xu X., 2019. Application of droplet digital PCR in detection of seed-transmitted pathogen *Acidovorax citrulli*. *Journal of Integrative Agriculture* 19: 561–569. DOI: 10.1016/S2095-3119(19)62673-0

Maheshwari Y., Selvaraj V., Hajeri S., Yokomi R., 2017. Application of droplet digital PCR for quantitative detection of *Spiroplasma citri* in comparison with real time PCR. *PLoS One* 12: e0184751. DOI: 10.1371/journal.pone.0184751

Mangolini A., Ferracin M., Zanzi M.V., Saccenti E., Ebnaod S.O., (…), Negrini M., 2015. Diagnostic and prognostic microRNAs in the serum of breast cancer patients measured by droplet digital PCR. *Biomarker Research* 6: 3–12. DOI: 10.1186/s40364-015-0037-0

Mansfield J., Genin S., Magori S., Citovsky V., Sriariyanum M., (…), Foster G.D., 2012. Top 10 plant pathogenic bacteria in molecular plant pathology. *Molecular Plant Pathology* 13: 614–629. DOI: 10.1111/j.1364-3703.2012.00804.x

Migliorini D., Pecori F., Raio A., Luchi N., Rizzo D., (…), Santini A., 2021. First report of *Erwinia amylovora* in Tuscany, Italy. *Phytopathologia Mediterranea* 60: 253-257. DOI: 10.36253/phyto-12817

NAPPO, Guidelines for the Movement of Propagative Plant Material of Stone Fruit, Pome Fruit, and Grapevine into a NAPPO Member Country. 2004.

OEPP/EPPO, 2019. PM 7/24 (4) *Xylella fastidiosa*. *Bulletin OEPP/EPPO Bulletin* 49(2): 175–227 DOI:10.1111/epp.12575

OEPP/EPPO, 2021 EPPO standard PM 1/2 (30) EPPO A1 and A2 lists of pests recommended for regulation as quarantine pests. 2021.

Passera A., Compant S., Casati P., Maturo M.G., Battelli G., (…), Mitter B., 2019. Not just a pathogen? Description of a plant-beneficial *Pseudomonas syringae* strain. *Frontiers in Microbiology* 10:1409. DOI: 10.3389/fmicb.2019.01409

Potnis N., Kandel P.P., Merfa M.V., Retchless A.C., Parker J.K., (…), De La Fuente L., 2019. Patterns of inter- and intrasubspecific homologous recombination inform eco-evolutionary dynamics of *Xylella fastidiosa*. *ISME Journal* 13: 2319–2333. DOI: 10.1038/s41396-019-0423-y

Purcell A.H., 1979. Control of the blue-green sharpshooter and effects on the spread of Pierce's disease of grapevines. *Journal of Economical Entomology* 72: 887–892.

Redak P.A., Purcell A.H., Lopes J.R.S., Blua M.J., Mizell III R.F., Andersen P.C., 2004. The biology of xylem fluid-feeding insect vectors of *Xylella fastidiosa* and their relation to disease epidemiology. *Annual Review of Entomology* 49: 243–270.

Regulation (EU) 2016/2031 of the European Parliament of the Council on protective measures against pests of plants, amending Regulations (EU) No 228/2013, (EU) No 652/2014 and (EU) No 1143/2014 of the European Parliament and of the Council and repealing Council Directives 69/464/EEC, 74/647/EEC, 93/85/EEC, 98/57/EC, 2000/29/EC, 2006/91/EC and 2007/33/EC. 26 October 2016

Rodriguez C.M., Obando J.J., Villalobos W., Moreira L., Rivera C., 2007. First report of *Xylella fastidiosa* infecting coffee in Costa Rica. *Plant Disease* 85: 1027. DOI: 10.1094/PDIS.2001.85.9.1027A

Saponari M., Boscia D., Nigro F., Martelli G.P., 2013. Identification of DNA sequences related to *Xylella fastidiosa* in oleander, almond and olive trees exhibiting leaf scorch symptoms in Apulia (Southern Italy). *Journal of Plant Pathology* 94: 688. DOI: 10.4454/JPP.V95I3.035

Saponari M., Boscia D., Altamura G., Loconsole G., Zicca S., (…), Martelli G.P., 2017. Isolation and pathogenicity of *Xylella fastidiosa* associated to the olive quick decline syndrome in southern Italy. *Scientific Reports* 7: 17723.

Sedlak R.H., Kuypers J., Jerome K.R., 2014. A multiplexed droplet digital PCR assay performs better than qPCR

on inhibition prone samples. *Diagnostic Microbiology and Infectious Diseases* 80: 285–286. DOI: 10.1016/j.diagmicrobio.2014.09.004

Selvaraj V., Maheshwari Y., Hajeri S., Yokomi R., 2019. Droplet Digital PCR for absolute quantification of plant pathogens. Pages 583-585 In: *Plant Biotechnology: Progress in Genomic Era*, (Khurana, S.M.P. and Gaur, R.K. ed.), Springer Nature, Singapore.

Sicard A., Zeilinger A.R., Vanhove M., Schartel T.E., Beal D.J., Daugherty M.P., Almeida R.P.P., 2018. *Xylella fastidiosa*: insights into an emerging plant pathogen. *Annual Review of Phytopathology* 56: 181–202. DOI: 10.1146/annurev-phyto-080417-045849

Thorne E.T., Stevenson J.F., Rost T.L., Labavitch J.M., Matthews M.A., 2006. Pierce's disease symptoms: comparison with symptoms of water deficit and the impact of water deficits. *American Journal of Enology and Viticulture* 57: 1–11.

Vanhove M., Retchless A.C., Sicard A., Rieux A., Coletta-Filho H.D., (…), Almeida R.P.P., 2019. Genomic diversity and recombination among *Xylella fastidiosa* subspecies. *Applied and Environmental Microbiology* 85: e02972-18. DOI: 10.1128/AEM.02972-18

Wells J.M., Raju B.C., Hung H.Y., Weisburg W.G., Mandelco-Paul L., Brenner D.J., 1987. *Xylella fastidiosa* gen. nov., sp. Nov: Gram-negative, xylem-limited, fastidious plant bacteria related to *Xanthomonas* spp. *International Journal of Systematic and Evolutionary Microbiology* 37: 136–147. DOI: 10.1099/00207713-37-2-136

Zhao Y., Xia Q., Yin Y., Wang Z., 2016. Comparison of droplet digital PCR and quantitative PCR assays for quantitative detection of *Xanthomonas citri* Subsp. *citri*. *PLoS One* 11: e0159004. DOI: 10.1371/journal.pone.0159004